International Journal of Biological Macromolecules 128 (2019) 391–400

Contents lists available at ScienceDirect

International Journal of Biological Macromolecules

journal homepage: http://www.elsevier.com/locate/ijbiomac

Wheat straw extracted lignin in silver nanoparticles synthesis: Expanding its prophecy towards antineoplastic potency and hydrogen peroxide sensing ability

Rijuta Ganesh Saratale [a], Ganesh Dattatraya Saratale [b], Gajanan Ghodake [c], Si-Kyung Cho [c], Avinash Kadam [a], Gopalakrishnan Kumar [d], Byong-Hun Jeon [e], Deepak Pant [f], Amit Bhatnagar [g], Han Seung Shin [b,*]

[a] Research Institute of Biotechnology and Medical Converged Science, Dongguk University-Seoul, Ilsandong-gu, Goyang-si, Gyeonggi-do 10326, Republic of Korea
[b] Department of Food Science and Biotechnology, Dongguk University-Seoul, Ilsandong-gu, Goyang-si, Gyeonggi-do 10326, Republic of Korea
[c] Department of Biological and Environmental Science, Dongguk University, Ilsandong-gu, Goyang-si, Gyonggido 10326, Republic of Korea
[d] Institute of Chemistry, Bioscience and Environmental Engineering, Faculty of Science and Technology, University of Stavanger, Box 8600 Forus, 4036 Stavanger, Norway
[e] Department of Earth Resources and Environmental Engineering, Hanyang University, Seoul 04763, Republic of Korea
[f] Separation and Conversion Technology, Flemish Institute for Technological Research (VITO), Boeretang 200, 2400 Mol, Belgium
[g] Department of Environmental and Biological Sciences, University of Eastern Finland, P.O. Box 1627, FI-70211 Kuopio, Finland

ARTICLE INFO

Article history:
Received 9 November 2018
Received in revised form 22 January 2019
Accepted 22 January 2019
Available online 23 January 2019

Keywords:
Lignin capped silver nanoparticles
Wheat straw
SKOV3 ovarian cancer cells
DPPH
H_2O_2 sensing
Minimum bactericidal concentration

ABSTRACT

Lignin, is the most abundant, renewable and degradable biopolymer available in the nature. The present study exploited purified lignin from wheat straw as reducing, capping and stabilizing agent for the green synthesis of silver nanoparticles (Li-AgNPs) under optimized conditions. The analytical studies revealed synthesized Li-AgNPs having a face centered cubic crystalline structure, size ranging ~15–20 nm and the biomolecules comprising majorly phenolic, hydroxyl and carboxylic group of lignin coated on the surface of AgNPs. Li-AgNPs showed significant antimicrobial efficacy against human pathogens namely; *Staphylococcus aureus* and *Escherichia coli* and also determined their minimum inhibitory and minimum bactericidal concentration (MIC and MBC). Li-AgNPs also displayed substantial antioxidant activity in terms of well-known enzyme marker viz.; ABTS and DPPH free radical scavenging assay relative to commercial AgNPs. In vitro cytotoxicity assay of Li-AgNPs demonstrated dose-dependent toxicity effects in SKOV3 ovarian cancer cell line (LD50; 150 μg/mL) indicative of promising anticancer agent. Further, H_2O_2 sensing ability of stabilized Li-AgNPs exhibited its vital role in determining reactive oxygen species. Synthesis of Li-AgNPs is a cheap green technology and could exhibit its commercial use in biomedical, cosmetic, and pharmaceutical industry.

1. Introduction

Lignin is the most renewable, non-toxic, highly branched aromatic natural biopolymer which is commonly observed in the middle lamella of plant cell wall. It contributes forte and stiffness to the plant cell walls, regulating the fluid flow and shielding the plant against biochemical attacks [1]. Lignin is a valuable byproduct of pulp and paper industries and is produced nearly 50 to 70 million tons per annum [2]. Because of more stable and complex chemical structure, lignin is considered as one of the most important biomolecule to produce fuels, as diverse applications in industry such as; paper, concrete additives, binders, paints, chemicals, dispersants, lubricants as well as in cosmetics [3–5]. Moreover, owing to its antioxidative and antimicrobial potential, lignin is broadly exploited for the synthesis of different biomaterials and extensively studied for drug delivery and tissue regeneration [6,7]. However, still lignin is an underutilized resource because of its certain properties such as, structural complexity, variable structure based on its source or separation methods, low solubility and miscibility [8].

Nanotechnology is gradually developing research area in materials science and has engaged a great attention in recent years because of its miscellaneous applications in various fields including; food, textile, electronics, agriculture, biosensors, and biomedical sector [9,10]. Silver nanoparticles (AgNPs) are widely utilized based on their exceptional catalytic activity, high surface area, chemical stability, conductivity and remarkable antimicrobial, anticancer, antidiabetic properties [11]. In case of AgNPs, biologically active silver (Ag^+) ions interact with bacterial cell wall, suppress DNA replication and finally lead to cell lysis and its detailed mechanism is reported in our recent study [12]. However, extensive use of AgNPs in various sectors releases same ions in the environment that leads to toxicity in living organisms of the ecosystem. There have been huge efforts devoted for the development of easy,

* Corresponding author.
E-mail address: spartan@dongguk.edu (H.S. Shin).

https://doi.org/10.1016/j.ijbiomac.2019.01.120
0141-8130/

clean, efficient, sustainable, and environmentally friendly procedure for NPs synthesis which follow green chemistry principles. This could be possible by using bio-based resources for the synthesis of NPs [13]. Lignin consists of many chemical functional groups for example carbonyl, phenolic, aliphatic hydroxyls, carboxyl and thiols acts as reducing agent besides potential capping and stabilizing matrix in green synthesis of AgNPs making the process more cost effective. There are few reports where Zimniewska et al. [14] synthesized lignin nanoparticles using ultrasonication by applying on linen fabric and observed that after treatment fiber attained ultraviolet radiation absorbing, antistatic, and antibacterial properties. Similarly, lignin NPs tailored with silver ions were coated on the textile fabric which showed higher antimicrobial activity with less environmental effect relative to metallic silver nanoparticles [1]. Rak et al., [4] synthesized Au, Rh, and Ru nanoparticles using lignin as a reducing and stabilizing agent.

Multidrug resistant bacteria (MDR) is one of the important issues in medical sector since these bacteria are resilient to most commercial antibiotics. In this regard, nowadays metal nanoparticles (particularly AgNPs) or NPs in combination with antibiotics have gained attention to improve antimicrobial properties against MDR [15]. Antioxidants play a crucial and protective role against the oxidative damage of the cell or cell organelle and thus combat over risk of chronic diseases [6]. Determination of free radical scavenging ability of synthesized Li-AgNPs increases its potential applications in medicinal, cosmetic and food processing. Cancer is one of the diseases having higher mortality rate worldwide and as stated by World Health Organization (WHO), it could reach 20 million new cases per year by 2025 [16]. The conventional treatment has certain drawbacks such as nonspecific target drug delivery, unendurable cytotoxicity to healthy cells and in general being more expensive. To avoid this, development of nanomaterials or nanocarriers for cancer recognition, diagnosis and treatment are attaining enormous interest worldwide [16,17].

Traditionally, hydrogen peroxide is used in bleaching and as food preservative to control the growth of microorganisms in food. However, elevated concentration of H_2O_2 enhances oxidative stress which leads to aging and cancer. In the current scenario, development of biosensors using enzymatic, non-enzymatic or analytical methods for H_2O_2 detection is studied very well [18,19]. Even though numerous procedures have been projected, yet there is an urgent need to develop a biosensor which should be reliable, selective, ecofriendly, and cost effective.

The present work was intended to explore the prospects of wheat straw lignin as a capping and stabilizing agent for silver nanoparticles synthesis to make the process more ecofriendly and cost effective. The effects of various influencing parameters were optimized to make the process more efficient and to produce even spherical silver nanoparticles in high yields. To explore the applicability of synthesized Li-AgNPs, antibacterial, and antioxidant activity were evaluated. In vitro cytotoxicity of Li-AgNPs against ovarian cancer SKOV3 cells was also investigated. Lastly, we have utilized the Li-AgNPs for colorimetric sensing of H_2O_2. This work is expected to offer worthwhile information for assessing the viability of wheat straw lignin for AgNPs synthesis and their biomedical, pharmaceutical and sensing applications.

2. Material and methods

2.1. Chemicals and reagents

Purified lignin extracted from wheat straw was employed as a preliminary material during the experiment of AgNPs synthesis. Silver nitrate ($AgNO_3$), sodium hydroxide, 3-[4,5-dimethylthiazol-2-yl]-2-5-diphenyltetrazolium (MTT), hydrogen peroxide (H_2O_2), gallic acid, ascorbic acid, potassium ferricyanide (III), dimethyl sulfoxide (DMSO), DPPH (2,2-diphenyl-1-picryhydrazyl), 2,2′-azino-bis(3-ethylbenzothiazoline)-6 sulphonic acid (ABTS), Folin–Ciocalteu's phenol reagent (2 N solution) were bought from Sigma-Aldrich, USA. All other chemicals required for all experiments were available with high purity and all are of analytical grade. Water filtered and purified by Milli-Q plus water purification system (Millipore Corporate, Billerica, MA) was used in the preparation of solutions during the whole experiment.

2.2. Lignin extraction from wheat straw

Wheat straw was obtained and kindly gifted by the local farmers of South Korea. The raw materials were dried for 10 to 12 h at 60 °C in an oven, milled, and passed through a sieve to achieve particles of ~1.0 mm size and stored in airtight container. The chemical constituents of wheat straw mainly cellulose 44.5 ± 2.65, hemicellulose 23.8 ± 1.90, and lignin 22.4 ± 1.85 was determined using the method stated earlier [20,21]. Lignin was extracted by alkali extraction method by adapting the procedure of [6]. In brief, 7.0 g of wheat straw powder was dewaxed by means of toluene-ethanol with 2:1 proportion (v/v) in soxhlet extraction apparatus and were treated by 2% NaOH aqueous solution at 120 °C for 45 min. The solid:liquid ratio was maintained with 1:10 (w/v) ratio. At the end of pretreatment, the mixtures were cooled to room temperature. The obtained dark brown colored liquor/fractions was filtered for the separation and further kept in oven (60 °C) for making it a concentrated solution. After the removal of hemicellulose, soluble alkali lignin fractions were isolated using repeated precipitation of lignin by maintaining the pH (1.5–2.0). The extracted lignin was meticulously rinsed using deionized water to get rid of the left over impurities and further utilized for AgNPs synthesis.

2.3. Chemical functional groups quantitative determination of extracted lignin

The total amount of carbohydrates present in lignin extracted fractions was measured by anthrone assay spectrophotometrically at 630 nm using glucose as standard [22]. Total soluble phenolic contents were measured using Folin–Ciocalteu test [23]. The reaction assay consists of extracted lignin (20 μL), distilled water (180 μL), Folin–Ciocalteu reagent (100 μL) and sodium carbonate (0.5 mL, 20%) solution. This mixture was mixed well in vortex machine, then it was covered and kept for 2 h at room temperature. By keeping gallic acid as the standard, the absorbance was monitored at 765 nm. The contents of total phenolic were stated as equivalents of gallic acid (μg per mg of dried sample). The concentration of hydroxyl phenolic units in lignin fractions was evaluated by following the procedure reported by [24]. Carboxyl groups in the extracted lignin were determined by suspending purified lignin sample about 100 mg in alkaline solution (100 mL; pH 12) and stirred for about 3 h. Then this mixture was titrated potentiometrically using hydrochloride acid (0.1 M) and calculated using the procedure reported [25].

2.4. Synthesis of Li-AgNPs and optimization of physicochemical parameters

To carry out the synthesis of AgNPs, $AgNO_3$ solution (1 mM) was dissolved in ultrapure water. The reaction solution consisted of lignin solution (0.02%) (3 mL) and then mixed in $AgNO_3$ solution (27 mL). This mixture was further maintained in water bath at 50 °C for 60 min. The influence of several physicochemical parameters such as pH (2.0, 3.0, 5.0, 6.0, 7.0, 8.0, 9.0, and 10.0), temperature (30, 40, 45, 50, and 60 °C), $AgNO_3$ concentration (0.5, 1.0, 2.0, and 3.0 mM) and incubation time (0, 30, 60, 90 and 120 min) on AgNPs synthesis using lignin was studied. The influence of lignin concentration using diverse mixing ratios of Li: $AgNO_3$ (1:1, 1:3, 1:5, 1:8, 1:10, 1:15, and 1:20) were systematically investigated. The process parameters were differed one at a time by keeping the other variables fixed. To determine the stability of synthesized Li-AgNPs, the samples were observed up to 3 months keeping them at room temperature conditions. The synthesized Li-AgNPs were checked for a variation in their surface plasmon resonance (SPR) through UV–vis measurements at different time intervals before and after 3 months. All experiments were repeated at least three times.

Table 1
Determination of total carbohydrates, phenolic hydroxyl group, carboxyl group and total phenolic content of extracted wheat straw lignin.

Sr. no	Lignin chemical composition studied	Concentration
1	Total carbohydrate content (mg/g)	0.92 ± 0.08
2	Phenolic hydroxyl group (%)	1.15 ± 0.04
3	Carboxyl group (%, w/w)	2.35 ± 0.12
4	Total phenolic content[a]	140.6 ± 5.6

Values are means of three replicates ± SE.
[a] Total phenol content determined as concentration of polyphenol (μg) in term of gallic acid equivalent per mg of extracted wheat straw lignin.

2.5. Characterization of synthesized Li-AgNPs

Reduction of silver ions (Ag^{+}) to AgNPs using lignin and time point of higher generation of Li-AgNPs was observed by measuring periodic scan of optical absorbance of the reaction mixture between 300 and 700 nm using UV–visible spectrophotometer (Optizen, Model 2120 UV plus). X-ray diffraction (XRD) was accomplished through Rigaku (Japan) X-ray diffractometer with 2θ scans starting at 20 to 80° at 0.04° per min with a time constant of 2 s. Fourier transform infrared (FT-IR) spectra analysis was performed between 4000 and 400 cm^{-1} with 4 cm^{-1} resolution speed by Perkin Elmer, Norwalk, CT, USA to determine the functional groups existing in lignin accountable for the reduction and stabilization of Li-AgNPs. To analyze element compositional content, energy dispersive analysis of X-ray spectroscopy were obtained by EDX, JEOL-64000, Japan. Zeta potential analysis of dispersed synthesized Li-AgNPs in deionized water in absence of any electrolyte was evaluated by ELS-8000 (OTSUKA Ltd., Japan). The Li-AgNPs were examined to study its surface morphology and shape by a high-resolution transmission electron microscopy (HR-TEM) images. The selective area diffraction patterns (SAED) for the samples were determined by means of a Tecnai G2 20 S-TWIN (FEI Company) instrument. The particle size dispersal and usual particle size of the Li-AgNPs was graphically presented by counting 100 distinct particles manually from TEM images.

2.6. Antioxidant activity of synthesized Li-AgNPs

The antioxidant activity of the Li-AgNPs was assessed with marker enzymes; 1,1-diphenyl-2-picrylhydrazyl (DPPH) free radical scavenging, and 2,2′-azino-bis (3-ethylbenzothiazoline-6-sulphonic acid) (ABTS) radical scavenging protocols. The antioxidant activity of biosynthesized sample against DPPH radical scavenging was investigated by following the method described by Saratale et al. [12]. For the assay, different concentrations of Li-AgNPs were chosen ranging from 10 to 100 μg/mL and catechol as the reference standard was used. Absorbance of the reaction mixtures was taken at 517 nm. The ABTS radical scavenging activity of Li-AgNPs was examined by applying standard procedure [26]. In short, 2 mL of solution of Li-AgNPs having

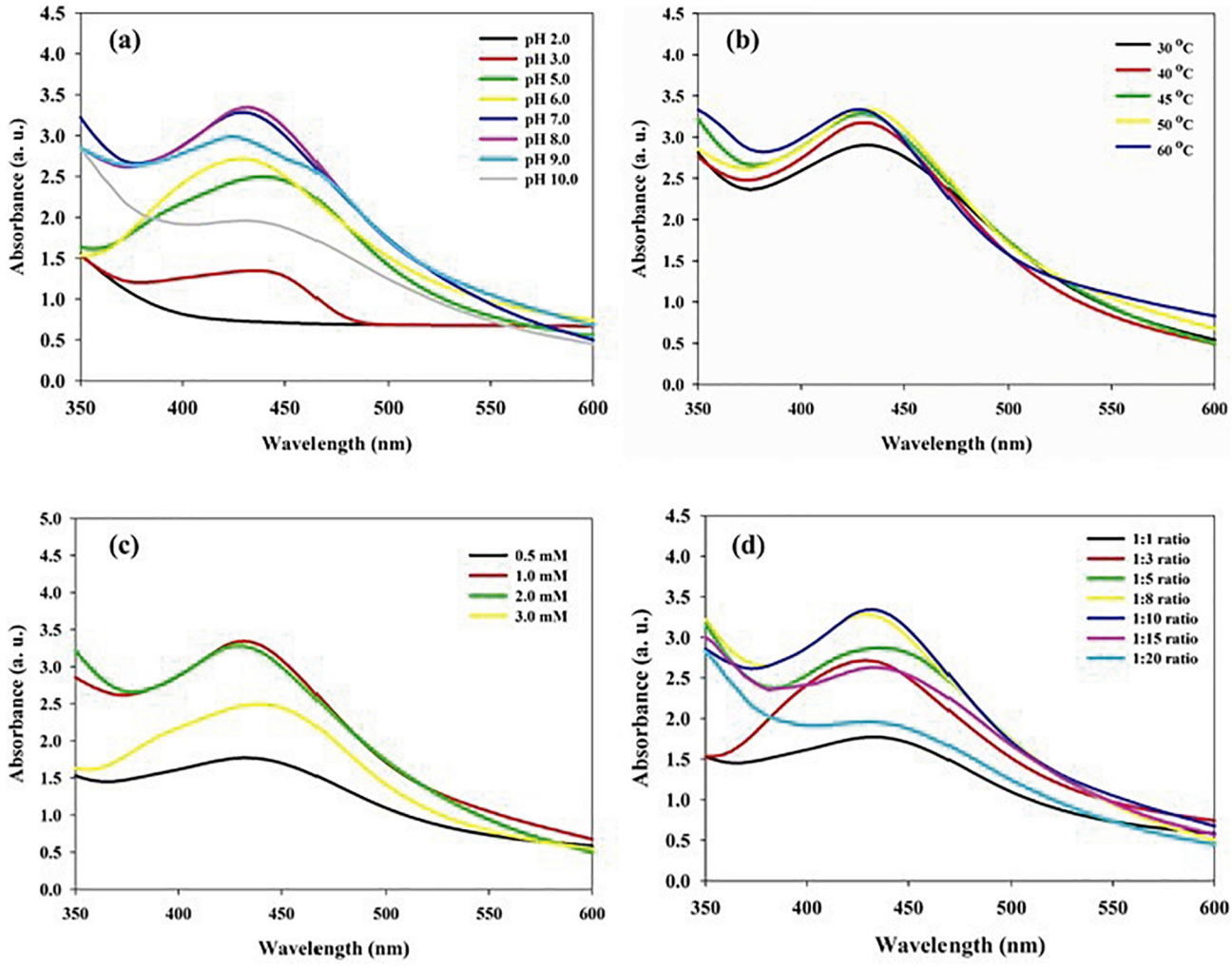

Fig. 1. UV–vis spectral analysis of AgNPs synthesized using wheat straw lignin at various reaction conditions: (a) initial pH; (b) incubation temperature; (c) $AgNO_3$ concentration and (d) Li:$AgNO_3$ ratio.

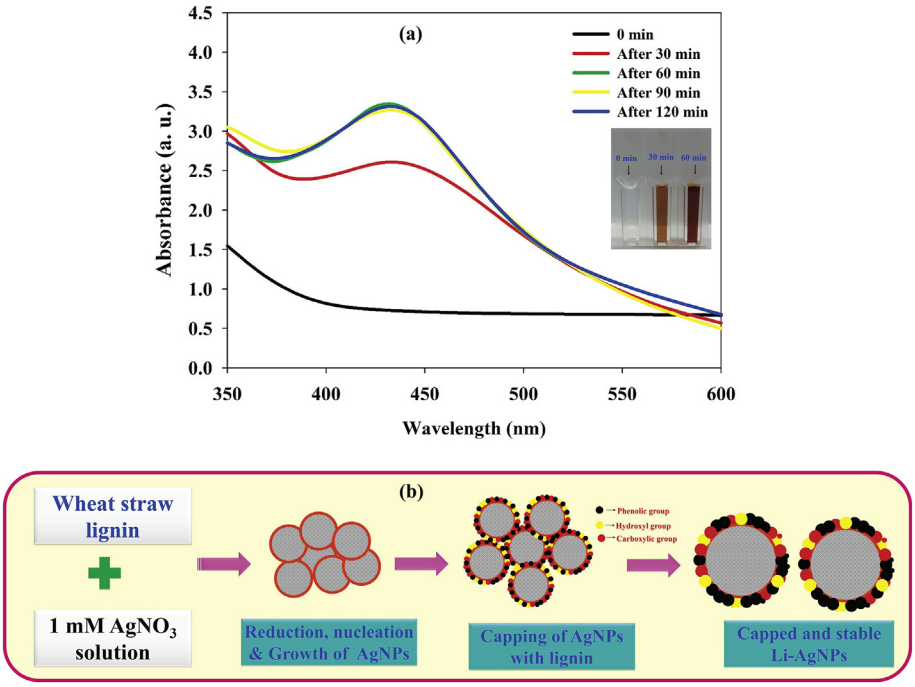

Fig. 2. (a) Effect of different incubation time under optimized conditions on SPR of Li-AgNPs (inset is digital pictures of the conforming AgNPs); and (b) possible mechanism of Li-AgNPs synthesis using lignin extracted from wheat straw.

varied concentrations (10 to 100 μg/mL) was mixed with 2 mL of solution of $ABTS^{+}$ and then vortexed for 10 s immediately and after 6 min. Then, the absorbance was measured at 734 nm by keeping ascorbic acid as a standard on spectrophotometer. The DPPH and ABTS free radical scavenging activity using standard AgNPs were also determined.

Each assay consists of a blank (without NPs) was always used. In all assays, mean and standard deviation ($n = 3$) were determined. The results were stated as the IC_{50} values (defined as the effective concentration which exhibit 50% inhibition of activity).

$$\text{Free radical scavenging } \% = \frac{[AC-AT]}{AC} \times 100$$

where, AC is the absorbance of the control in the respective assays, and AT is the absorbance of treatment using Li-AgNPs.

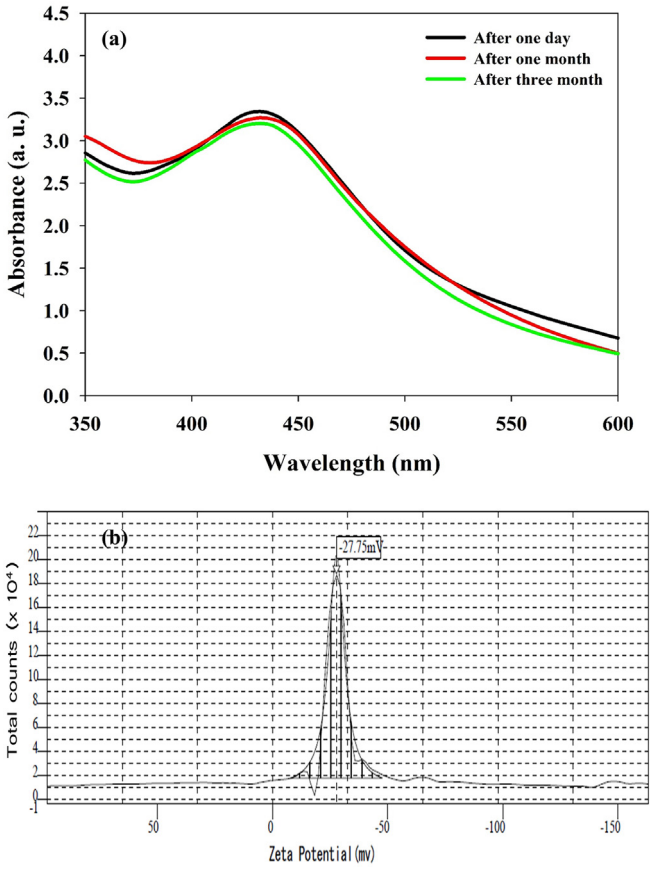

Fig. 3. (a) stability of synthesized Li-AgNPs up to three months and their SPR spectrum at different time intervals and (b) zeta potential of the synthesized Li-AgNPs.

2.7. In vitro cell cytotoxicity in SKOV3 ovarian cancer cells

In vitro cytotoxic effect of synthesized Li-AgNPs was investigated using SKOV3 cancer cell line by MTT assay [27]. SKOV3 cells were obtained from the American type culture collection (Manassas, VA). Using 96-well microliter plates, about 1×10^4 cells/well were achieved in 24 h. Cells were seeded in Dulbecco's modified Eagle's medium (DMEM) having streptomycin 100 μl, FBS 10%, penicillin 100 U/mL, and further cultivated for 24 h at 37 °C in 5% CO_2 atmosphere incubator to attain the adherence to polystyrene microplates. Further, the cells were cultured at 37 °C, 5% CO_2 for 72 h. Viabilities of the cultured cell was measured by MTT assay according to manufacturer's instructions. Set of control, well-known anticancer drug, doxorubicin (Dox) at 25 μg/mL concentration and lignin were assayed. Lastly, the cell viabilities for all the sets were determined by measuring the absorbance (also for the blanks) at 590 nm in a multi well ELISA plate reader (Biotek, Epoch microplate spectrophotometer, Winooski, USA). The percentage (%) of cell viability was measured using the formula reported [11].

2.8. Antibacterial efficacy of synthesized Li-AgNPs against human pathogens

To evaluate the antimicrobial efficacy of extracted lignin and elevated concentrations of Li-AgNPs (10, 20, and 30 μg/mL) was accomplished using agar disc diffusion method [28]. Two human pathogenic

strains, *Staphylococcus aureus* and *Escherichia coli* were studied. Luria–Bertani (LB) medium was used for culturing the strains. Both the bacterial culture (100 μL) were grown overnight and equally spread on the surface of sterile agar plates (LB medium) with the help of a sterilized cotton swab. The minimum inhibitory (MIC) and minimum bactericidal concentration (MBC) were investigated by applying the procedure reported [12]. In this study, MIC and MBC concentration were measured in μg/mL. The combined in vitro antibacterial efficacy of Li-AgNPs, with regular market antibiotics for instance ampicillin, oxytetracycline, tetracycline, and streptomycin was checked for *S. aureus* and *E. coli* using the method and conditions described earlier [12]. The antibacterial potency of the Li-AgNPs was investigated by quantifying the inhibition zones diameter (mm) after incubating both plate and the liquid cultures at 30 °C in bacteriological incubator for 24 h. The diameter of 'zone of inhibition' at each well was calculated and noted. All experiments were performed at least three times. The combined antibacterial efficacy of the Li-AgNPs/antibiotics mixture was evaluated by measuring the escalation in the fold area of the zone of inhibition.

2.9. Hydrogen peroxide sensing ability of synthesized Li-AgNPs

The sensing ability of Li-AgNPs to sense H_2O_2, by following the procedure reported earlier [29]. Initially spectrum of Li-AgNPs solution (2 mL) was recorded using the UV–visible spectrophotometer. For H_2O_2 sensing the reaction conditions are; 0.8 mL of 100 μM of H_2O_2 and 0.2 mL of Li-AgNPs and then this solution was mixed vigorously. The reaction mixture was then retained at room temperature for 15 min, and the absorption spectra at regular time intervals within 300–800 nm were measured.

2.10. Statistical analysis

All measurements and assays were conducted in triplicates. All the data were evaluated using one-way analysis of variance (ANOVA) with a Tukey-Kramer multiple comparisons test.

3. Results and discussion

3.1. Determination of chemical constituents of purified wheat straw lignin

To understand the responsible chemical constituents available in purified wheat straw lignin, we have determined the total carbohydrates, phenolic hydroxyl group, carboxyl group and total phenolic content. It showed higher amount of phenolic content which is about (140.6 ± 5.6 μg GAE) whereas moderate phenolic hydroxyl and carboxyl groups are present. The observed total phenolic content was found comparable with lignin extracted from *Miscanthus sinensis* having 170–190 μg of GAE/mg of lignin [30]. In the extracted lignin, total carbohydrate was present in very little amount and the details of all other composition is summarized in Table 1. The foregoing results suggest that mainly the phenolic, carboxyl and hydroxyl group play a major role in the reduction, capping and stabilizing of AgNPs synthesis.

3.2. Optimization of various operational parameters for Li-AgNPs synthesis

Initially, we have optimized various reaction conditions such as; pH, incubation temperature, different concentration of silver nitrate, lignin concentration and incubation time to achieve maximum yield of lignin mediated AgNPs. It was observed that these factors are responsible for size and shape of AgNPs and their yield. The surface plasmon resonance (SPR) of AgNPs is subjective to the NPs agglomeration, its size, shape, and neighboring dielectric medium [27]. Thus, we have evaluated and checked the SPR at different optimizing conditions for the formation of Li-AgNPs which are presented in Fig. 1a–d. The initial pH value of reaction mixture ($AgNO_3$) plays a vivacious part in AgNPs synthesis as well as its size and shape. We have studied the effect of pH from acidic to alkaline condition i.e. from pH 2 to 10. At higher acidic condition, no SPR was observed however, at elevated pH, increase in broad spectrum of SPR can be seen (Fig. 1a). On the other hand, at neutral and slightly basic condition (pH 8.0) resulted in formation of dark brown color, strong and narrow peak at 432 nm which might be due to the reduced size and degree of anisotropy of the silver particles [31]. However, at above pH 8, a reduction in SPR spectrum was observed possibly due to the higher agglomeration of NPs. Even at higher alkaline pH (10.0) there was sharp reduction in SPR was recorded. The results suggest that pH 8.0 is the optimum condition for maximum Li-AgNPs production.

The influence of incubation temperature (30, 40, 45, 50, and 60 °C) on the production of Li-AgNPs was investigated. At temperature from 30 °C to 40 °C, lower SPR spectrum was observed whereas at elevated

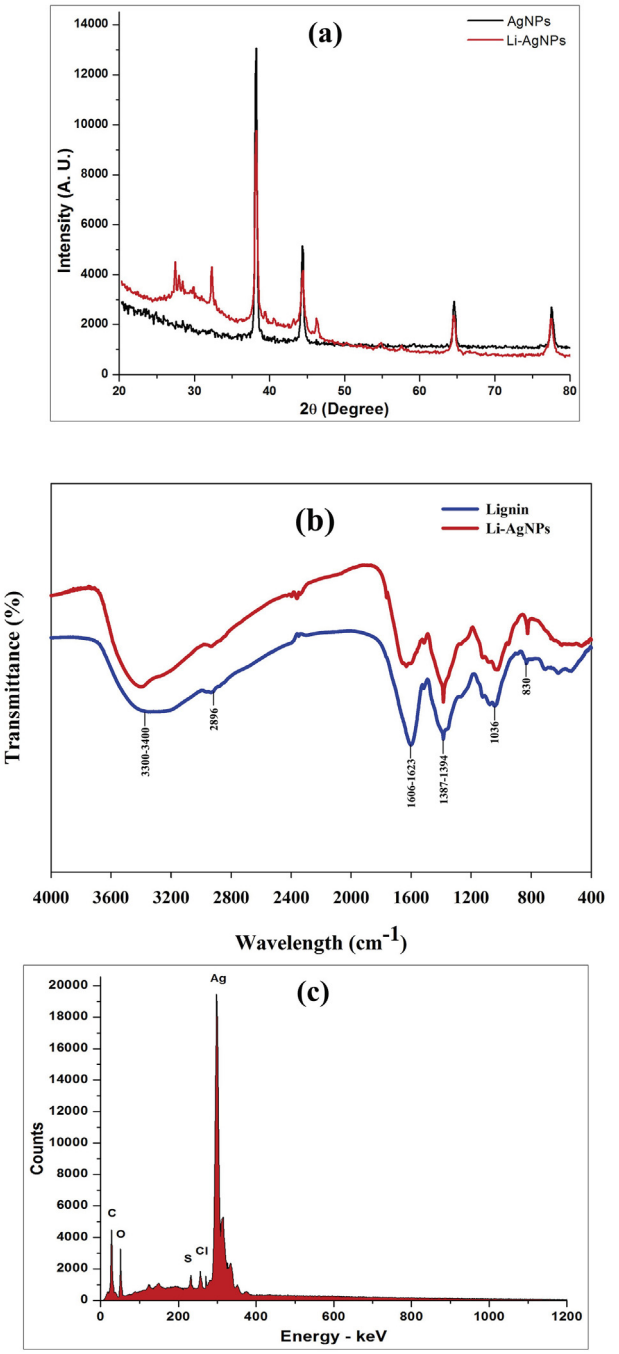

Fig. 4. (a) XRD pattern of AgNPs and Li-AgNPs; (b) FTIR spectra of lignin and Li-AgNPs; and (c) EDX spectrum; of the synthesized Li-AgNPs.

temperature SPR spectrum was increased and sharp band was observed indicating decrease in the particle size (Fig. 1b). However, little variation in SPR spectrum at 50 and 60 °C can be seen. To make the process less energy intensive, we have selected the reaction condition at temperature 50 °C. The influence of increasing silver nitrate ($AgNO_3$) concentration from 0.5 mM to 3.0 mM was determined by maintaining the other reaction conditions constant. There was a sharp increase in SPR peak from 0.5 to 1.0 mM concentration possibly as a result of elevated oxidation of hydroxyl groups by metal ions [32]. The obtained results are depicted in Fig. 1c. However, at elevated concentration, reduction in SPR was observed which could be due to the presence of higher amount of silver ions immersed on the surface of preordain nuclei that tends to result in formation of larger nanoparticles [31]. In addition, we have examined the effect of mixing different ratio of lignin and $AgNO_3$ (1 mM) solution (1:1, 1:3, 1:5, 1:8, 1:10, 1:15 and 1:20). The experimental results suggest that 1:10 mixing ratio of lignin: $AgNO_3$ was found optimum in which a sharp and higher SPR spectrum was recorded (Fig. 1d). Lower concentration of lignin is optimum indicating higher reducing capacity of wheat straw lignin for the increased reduction of silver ions [6]. However, very little particularly 1:15 and 1:20 lignin and $AgNO_3$ mixing ratio concentration was found not effective for the synthesis of Li-AgNPs which leads to reduction in SPR. The results also suggest that lignin concentration carry a crucial role in defining the progression and the size dispersal of AgNPs. The effects of different reaction time (0, 30, 60, 90 and 120 min) were investigated by keeping the other conditions constant in the synthesis of AgNPs. From the Fig. 2a, it can be seen that in relation with the time, a steady increase in the intensity of SPR peak at ca. 432 nm without any change in the peak wavelength up to 60 min indicated the formation of uniform particle shape. However, on incubating for long time (90 and 120 min), very slight change in SPR was observed which indicates that 60 min is the optimum incubation time to achieve maximum Li-AgNPs synthesis. The literature study showed that AgNPs have characteristic SPR band generally at wavelength in between from 400 to 480 nm [33], and the similar performance was also observed in the current investigation. Thus, from the above mentioned outcomes, the optimum reaction parameters were found are; incubation temperature: 50 °C, initial pH: 7.0, $AgNO_3$ concentration: 1.0 mM, Lignin/$AgNO_3$ ratio: 1:10, and the incubation time: 60 min which were used in the subsequent experiments.

Additionally, on the basis of the obtained analytical results, we have proposed the mechanism of Li-AgNPs synthesis that the lignin biochemical constituents mainly the phenolic, aliphatic hydroxyl and carboxylic groups acts as capping, reducing and stabilizing matrix for AgNPs. The possible reaction mechanism of lignin mediated AgNPs synthesis is schematically represented in Fig. 2b.

3.3. Stability of the synthesized Li-AgNPs

Li-AgNPs which were synthesized under the optimal reaction conditions were investigated to study its stability by storing them at ~30 °C for three months. After three months of storage, no particle aggregation was observed. Similarly, the SPR spectrum of synthesized Li-AgNPs was measured at 432 nm which was almost similar but with a slight reduction in peak intensity observed after 3 months of incubation (Fig. 3a). The zeta potential results of the synthesized Li-AgNPs are used to determine the surface charge which is vital factor to understand the interfaces between NPs and their extensive duration stability in liquid

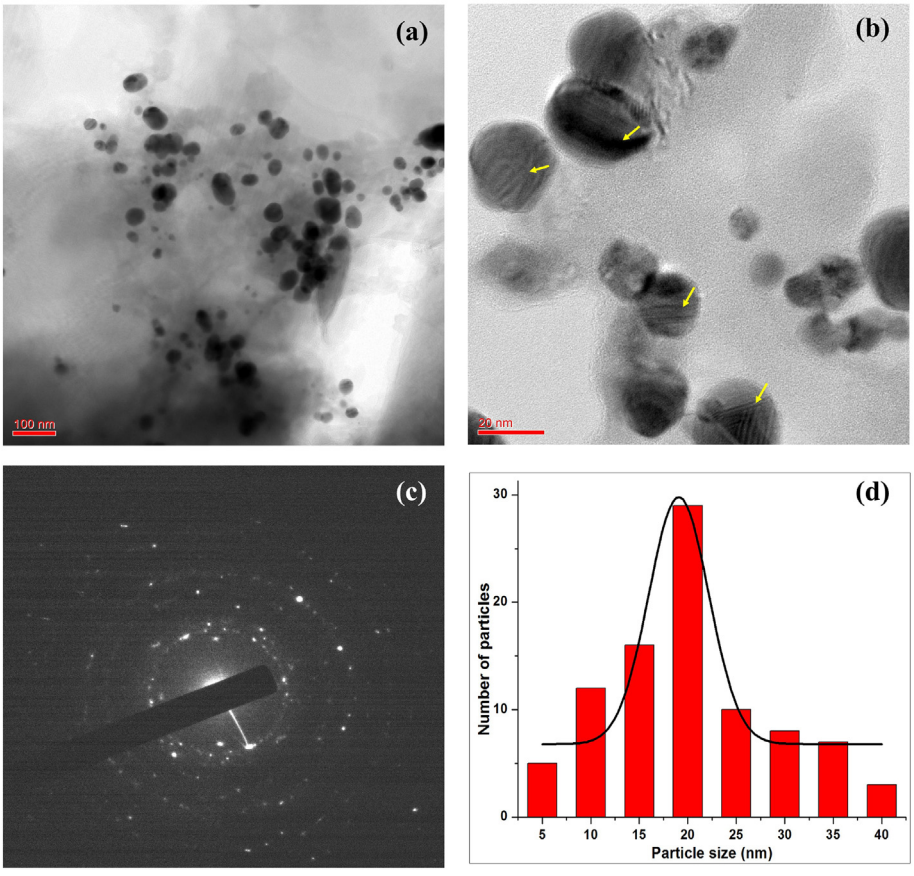

Fig. 5. HRTEM micrographs of Li-AgNPs (a) at 100 nm (b) at 20 nm magnification; (c) selected area diffraction pattern (SAED) and (d) average particle size histogram of the synthesized Li-AgNPs.

media. The zeta potential results of Li-AgNPs showed higher negative charge −27.75 mV (Fig. 3b). This negative charge on the surface of Li-AgNPs were suggestive that NPs repel each other, and prevent the agglomeration of NPs. Due to this property, our synthesized Li-AgNPs are suitable for long-term stability which support our results of stability of the synthesized Li-AgNPs (Fig. 3a). The foregoing results also confirmed that the lignin synthesized AgNPs were highly stable and increases its potential use in biomedical and sensing applications.

3.4. Characterization of the synthesized Li-AgNPs

The XRD spectrum of Li-AgNPs exhibited four diffraction peaks at 2θ (38.2°, 44.4°, 64.4°, and 77.5°) that relate to (111), (200), (220), and (311) which is similar to standard AgNPs (Fig. 4a). These values correlates with face centered cubic (fcc) structures of Ag as per the standard JCPDS no. 04-0783. The greater intensity of (111) reflection peak revealed the crystalline structure of Li-AgNPs. Moreover, along with the characteristic Bragg peaks of AgNPs some additional peaks, 2θ = 27.6° and 32.3° were also observed and indicative of reducing and capping agents of lignin molecule present on the surface of AgNPs. Similar reflection peaks were observed in the synthesis of AgNPs using pullulan [34] and dextran [35] biomolecule.

Fig. 4b represents the FTIR spectra of wheat straw lignin (Li) and lignin synthesized and capped AgNPs (Li-AgNPs). The bands at 3300–3400 cm^{-1} showed stretching of phenolic OH group. The band of Li-AgNPs at 3400 cm^{-1} became sharper and intense compared to the FTIR of lignin. Band with moderate intensity was obtained at 28960 cm^{-1} attributes to the stretching of CH in methyl groups of lignin. This peak was shifted to some extent in Li-AgNPs compared to lignin spectrum bands at 1606–1623 cm^{-1}. Further it showed higher intensity of aromatic skeleton vibration type of bands of lignin in both the samples which are concomitant with ring conjugated stretching of C═C was noticed in extracted lignin. Moderate intensity bands at 1387 cm^{-1}, 1394 cm^{-1} are mainly owing to aromatic skeleton vibration and O—CH_3, and the symmetry of C—H deformation [30]. The band between 1000 and 800 cm^{-1} were mostly attributed to aromatic vibrations groups of C═O, C—O, and C—H out of plane deformation and OH stretching of primary alcohol [6]. The earlier reports of Mohan et al. support our results and are in well agreement with the contention that the peak around 3400 cm^{-1} became shorter compared to control lignin. This variation in peak intensity can occur due to the electrostatic cross-binding among lignin and AgNPs [6,36]. FTIR results confirmed that the diverse functional groups of lignin (carboxyl, carbonyls, phenolic and aliphatic hydroxyls, etc.) are accountable for the silver ions reduction. In addition, it has been reported that these biomolecules creates a protective surrounding on the AgNPs surface and thus stabilize the synthesized AgNPs by forming a steric hindrance around the AgNPs [31,37].

The EDX spectrum of Li-AgNPs displayed the strong prominent peak at 3 keV, the representative absorption SPR of metallic silver with higher proportion and also gave the details of quantitative status of other elements (Fig. 4c). In EDX spectrum, along with Ag minor peaks conforming to C, O, S and Cl confirmed the presence of chemical constituents of lignin on the surface of the synthesized Li-AgNPs (Fig. 4c).

3.5. Morphological analysis of Li-AgNPs using HR-TEM

HR-TEM analysis showed that Li-AgNPs are uniformly mono dispersed and are spherical shaped NPs (Fig. 5a and b). At higher magnification dispersed AgNPs showed fringes in black colored can be perceived which specifies that different functional groups or chemicals of lignin are present on the surface of the synthesized AgNPs (Fig. 5b). Moreover, small agglomeration of AgNPs can be seen and this may be possibly due to the interaction of lignin molecules existent on the surface of Li-AgNPs. The SAED pattern exhibited the intensively polycrystalline nature of the AgNPs which comply with lattice planes of Bragg's reflection (111), (200), (220) and (311) planes in agreement with the XRD results (Fig. 5c). The particles histogram disclosed the average particle size of nearly ~20 nm (Fig. 5d).

3.6. Antioxidant assays (DPPH and ABTS) of Li-AgNPs

Lignin is well known free radical scavenger that reduces the oxygen radicals' concentration and inhibits the oxidation reactions. The antioxidant activity of produced Li-AgNPs was assessed by using two in vitro methods such as DPPH and ABTS radical scavenging assays. DPPH capability of Li-AgNPs, lignin, AgNPs only and catechol as a standard were investigated and the IC_{50} value of antioxidant potential is indicated in Fig. 6a. The AgNPs showed substantial DPPH radical scavenging potential with IC_{50} value of 72.30 μg/mL which is substantially greater than IC_{50} value of AgNPs and the lignin 112 μg/mL and 150 μg/mL, respectively (Fig. 6a). The activity of DPPH assay of Li-AgNPs was found to be dose reliant and maximum inhibition about 62.5 at 100 μg/mL and upon further elevation in the concentration, there is no substantial increase in the activity was observed. Li-AgNPs displayed significant ABTS radical scavenging activity with less value of IC_{50} value of 52.8 μg/mL which is comparable with standard ascorbic acid (IC_{50} 72.30 μg/mL) and considerably greater than lignin (IC_{50} 125.4 μg/mL) and AgNPs (IC_{50} 86.5 μg/mL) (Fig. 6b). The difference in free radical scavenging potential of Li-AgNPs because of their variable reactivity against the DPPH and ABTS. In our study, Li-AgNPs displayed higher free radical scavenging activity in both the cases as compared to sole lignin. The

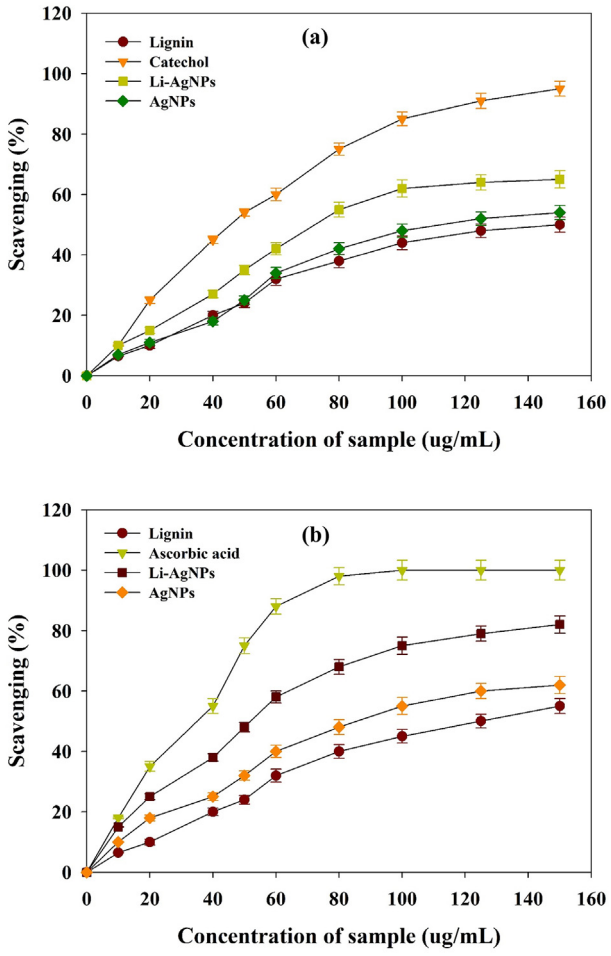

Fig. 6. Antioxidant potentials of synthesized Li-AgNPs in terms of free radical scavenging activity; (a) DPPH radical scavenging; (b) ABTS radical scavenging at various concentration.

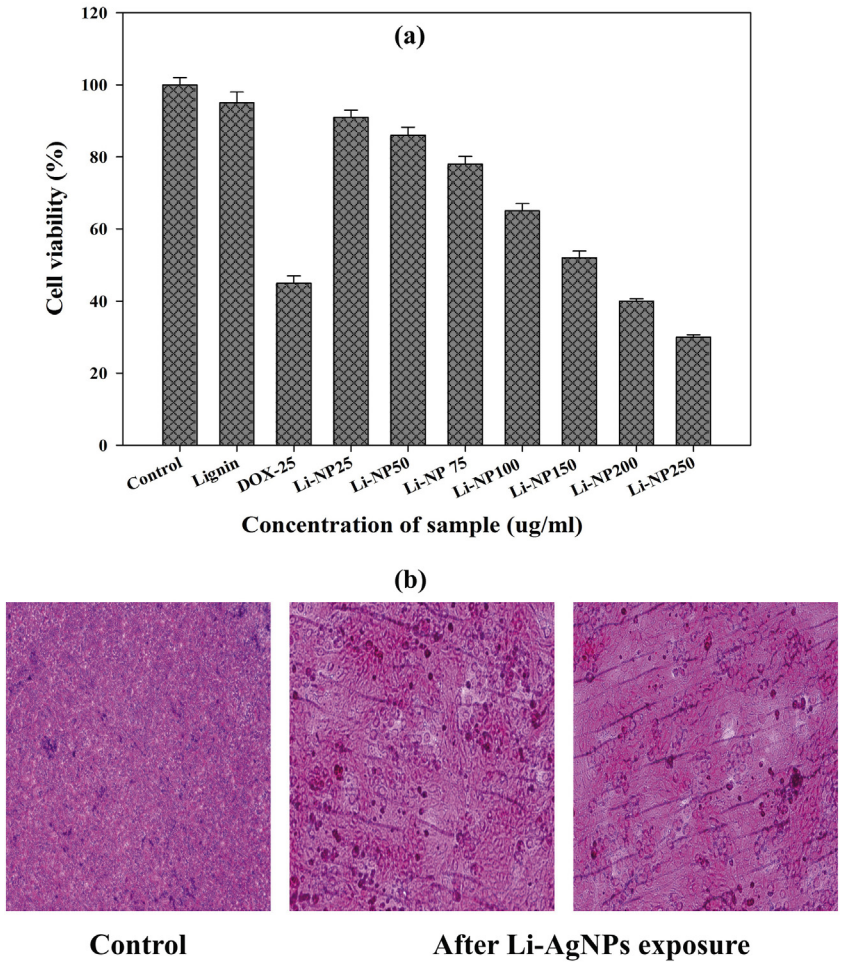

Fig. 7. (a) In vitro cytotoxicity of synthesized Li-AgNPs at various concentrations against ovarian cancer cell line SKOV3 (DOX-25: standard anticancer drug doxorubicin at concentration of 25 μg/mL); and (b) images of SKOV3 cells before (control) and after Li-AgNPs treatment.

reason for this significant activity is that Ag acts as a strong oxidant and have ability to lose electrons easily was reported recently [38]. The enhancement in the activity of Li-AgNPs relative to lignin and AgNPs only which might be because of capping of AgNPs with biomolecules of lignin mainly higher phenolic hydroxyl groups, and aliphatic hydroxyl groups was also ascertained through FTIR analysis. Similar results were observed in case of *Pongamia pinnata* leaf extract mediated AgNPs where synthesized AgNPs showed better antioxidant activity relative to chemically synthesized AgNPs [39]. The foregoing results suggest that Li-AgNPs have significant antioxidant potential and thus could be useful to develop or configure new-fangled pharmaceutical products.

3.7. Antineoplastic potential of Li-AgNPs against SKOV3 ovarian cancer cell line

In vitro cytotoxicity effect of stable lignin capped AgNPs was studied against SKOV3 ovarian cancer cell lines and cell viability was studied using MTT assay. The AgNPs were found capable to decline SKOV3 cell viability in a dose-reliant mode as presented in Fig. 7a. To achieve half-maximal inhibition response (IC_{50}) of the SKOV3 cell viability using Li-AgNPs were intended graphically and showed the value as 150 μg/mL and at increased concentration of 250 μg/mL about 70%

Table 2
Antibacterial potential of lignin and Li-AgNPs against human pathogens *Escherichia coli* and *Staphylococcus aureus* and determination of their MIC and MBC.

Escherichia coli		*Staphylococcus aureus*	
AgNPs concentration (μg/mL)	Zone of inhibition (mm)	AgNPs concentration (μg/mL)	Zone of inhibition (mm)
Lignin	2.8 ± 0.15	Lignin	2.0 ± 0.12
10	9.30 ± 0.65	10	8.52 ± 0.44
20	11.28 ± 0.84	20	9.48 ± 0.55
30	12.50 ± 0.75	30	10.9 ± 0.60
MIC concentration	20.0 ± 1.22 μg/mL	MIC concentration	25.0 ± 1.54 μg/mL
MBC concentration	25.0 ± 1.45 μg/mL	MBC concentration	30.0 ± 2.22 μg/mL

Values are means of three replicates ± SE.
MIC - minimum inhibitory concentration; MBC - minimum bactericidal concentration.

Table 3
Synergistic antibacterial potential of Li-AgNPs and in combination with standard antibiotics, (oxy-tetracycline, tetracycline ampicillin and streptomycin,) against *Escherichia coli* and *Staphylococcus aureus*.

Antibiotic concentration (μg)	*Escherichia coli*		*Staphylococcus aureus*	
	ZOI (mm)		ZOI (mm)	
	Ab	Ab + Li-AgNPs	Ab	Ab + Li-AgNPs
Oxy-tetracycline	13.6 ± 1.12	19.7 ± 1.24	16.2 ± 0.92	23.2 ± 1.15
Tetracycline	14.6 ± 0.95	18.25 ± 0.84	14.3 ± 0.85	18.8 ± 1.05
Ampicillin	15.8 ± 0.84	18.9 ± 0.90	13.4 ± 0.88	16.2 ± 0.92
Streptomycin	14.8 ± 0.75	21.5 ± 1.22	15.3 ± 1.05	22.2 ± 1.25

Values are means of three replicates ± SE.
Ab - antibiotic.

inhibition was recorded (Fig. 7a). The actual cell images before and after Li-AgNPs exposure are shown in Fig. 7b which showed dose dependent ($P < 0.05$) cytotoxicity against SKOV3 cell. Sole lignin showed 5% inhibition whereas commercial anticancer drug doxorubicin at 25 μg/mL showed 55% inhibition. The obtained anticancer activity of Li-AgNPs was as good as to commercial cytotoxic agents and is notable. Numerous studies of in vitro show AgNPs were found toxic to mammalian cells. Herein, we firstly report the cytotoxic effects of Li-AgNPs in SKOV3 ovarian carcinoma cells but still more detailed study is required to explore detailed mechanism behind this anticancer effect.

3.8. Antibacterial activity of Li-AgNPs against human pathogens

Initially, we have checked the antibacterial activity of lignin and elevated concentration of Li-AgNPs (10 to 30 μg/disc) in contradiction of human pathogens namely *E. coli* and *S. aureus* (Table 2). The results suggest that Li-AgNPs showed noteworthy antibacterial potential against selected human pathogens with increase in zones of inhibition (ZOI). However, solitary lignin exhibited less effect against both the microbial strains. The results are depicted in Table 2. We have also determined the values of MIC and the MBC of Li-AgNPs against *E. coli* and *S. aureus.* For *E. coli*, MIC value was lesser (20 μg/mL) relative to MIC value (25 μg/mL) of *S. aureus* however, MBC value for *E. coli* (25 μg/mL) and for *S. aureus* (30 μg/mL) which was marginally greater compared to value of MIC in both the strains (Table 2). The synergistic antibacterial potency of Li-AgNPs with commercial antibiotics against *E. coli* and *S. aureus* was determined. The results suggested that Li-AgNPs in combination with oxytetracycline and streptomycin showed significant inhibition (45%) and increase in ZOI was recorded. However, other symbiotic antibiotic formulation was found less effective against both the strains (Table 3). The synergistic antibacterial performance of the Li-AgNPs and their obtained potential outcomes are presented in (Table 3). Li-AgNPs in combination with standard antibiotic leads to higher diffusion and destruction of bacterial cell membrane and cell organelle resulting in death of bacteria. Thus, this combination could be useful to abate the widespread practice of antibiotics against MDR and to be used as a potential antibacterial drugs.

3.9. Li-AgNPs colorimetric sensing of hydrogen peroxide and its selectivity

The ability of Li-AgNPs for colorimetric sensing H_2O_2 was also determined. After addition of 100 μM of H_2O_2 there was a sharp reduction in absorbance of SPR at 432 nm with transformation in color of the solution from dark brown to colorless solution within 15 min being observed (Fig. 8a). Moreover, to develop an optical sensor, selectivity is an important issue [40]. Considering this, we have checked the selectivity assay with concomitant species for instance, Co(II), Mn(II), Cu(II), Cr (III), Mg (II), Fe(II), Br^-, Ca(II), and glucose at higher concentration (0.1 mM). In the presence of these species there was very little difference in the spectral profile in relative to significant alteration when H_2O_2 was added (Fig. 8b). The results entail the high selectivity of Li-AgNPs for the sensing H_2O_2 colorimetrically. It was supposed that after addition of H_2O_2, it produces highly reactive oxygen radicals which destructs the Li-AgNPs and leads to the aggregation of the nanoparticles. A probable reaction route of catalytic activity of Li-AgNPs and H_2O_2 is depicted in Fig. 8c. The surface morphology plays a significant role in the sensitivity of the assay. The decrease in absorbance is because of morphological changes which were supported by TEM analysis where there is sharp reduction in size from ~20 nm to about ~8 to 9 nm (data not shown). The foregoing results are supporting the probable mechanism of H_2O_2 sensing by synthesized Li-AgNPs. Recently Cai et al., [41] developed bacterial cellulose mediated $Ni(OH)_2$ paper as potential supercapacitor electrode and also utilized for highly sensitive H_2O_2 detection. The sensing ability of our Li-AgNPs showed high sensitivity and selectivity for H_2O_2 compared to other studies [42] which increases the importance and its practical application. However, further research will be devoted towards the application of Li-AgNPs for sensing H_2O_2 and toxic compounds in market products and their quantification.

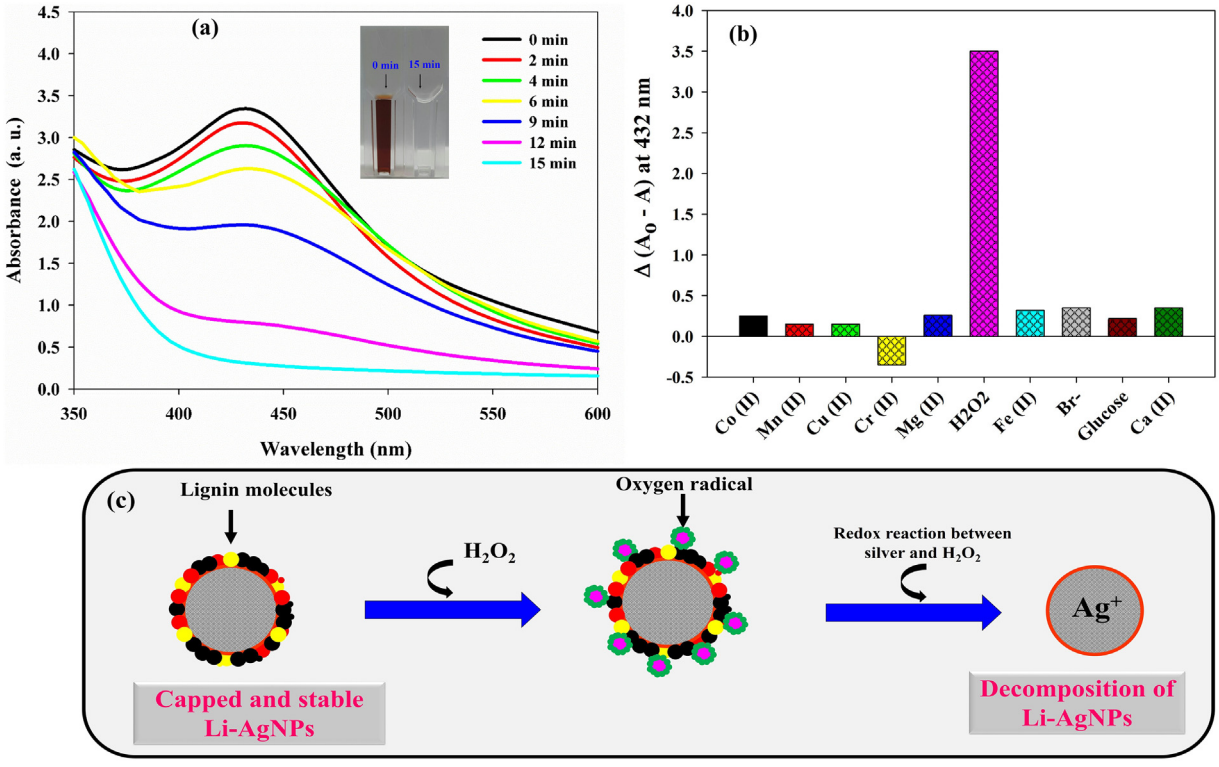

Fig. 8. (a) Optical spectra elucidating Li-AgNPs colorimetric sensing of H_2O_2 (100 μM) as a function of time, inset is the actual photograph viewing the visible color transformation after addition of H_2O_2; (b) selectivity of Li-AgNPs to H_2O_2; and (c) probable reaction mechanism of sensing H_2O_2 by Li-AgNPs.

4. Conclusions

Lignin mediated one step silver nanoparticles synthesis process was developed and is simple, ecofriendly follows the principles of green chemistry. The biomolecules of lignin acts as capping and stabilizing matrix for AgNPs. Li-AgNPs showed higher antibacterial potential against human pathogens and also displayed synergistic antibacterial effect with antibiotics. Significant antioxidant activity and dose dependent cytotoxicity against SKOV3 ovarian cancer cell increases its practice in medical sciences. The Li-AgNPs showed high sensing and selective ability towards H_2O_2. Developing optical sensor using Li-AgNPs would be easy, sustainable and inexpensive approach to detect reactive species and toxic chemicals increasing its application in industrial sector.

Acknowledgements

The authors gratefully acknowledge the research support by Dongguk University, South Korea under research fund 2018–2020. Authors are thankful to Dr. So Hyun Moon for her kind help during anticancer studies and Prof. Shrikrishna D. Sartale, Savitribai Phule Pune University, Pune, India for his help for the analytical studies. This work was supported by Korea Institute of Planning and Evaluation for Technology in Food, Agriculture, Forestry and Fisheries (IPET) through High Value-added Food Technology Development Program funded by Ministry of Agriculture, Food and Rural Affairs (MAFRA)(118056-2) and funded by Korea Environmental Industry & Technology Institute (A117-00197-0703-0).

References

[1] A.P. Richter, J.S. Brown, B. Bharti, A. Wang, S. Gangwal, K. Houck, E.A. Cohen Hubal, V.N. Paunov, S.D. Stoyanov, O.D. Velev, An environmentally benign antimicrobial nanoparticle based on a silver-infused lignin core, Nat. Nanotechnol. 10 (2015) 817–823.
[2] J. Zeng, Z. Tong, L. Wang, J.Y. Zhu, L. Ingram, Isolation and structural characterization of sugarcane bagasse lignin after dilute phosphoric acid plus steam explosion pretreatment and its effect on cellulose hydrolysis, Bioresour. Technol. 154 (2014) 274–281.
[3] W. Yang, J.M. Kenny, D. Puglia, Structure and properties of biodegradable wheat gluten bionanocomposites containing lignin nanoparticles, Ind. Crop. Prod. 74 (2015) 348–356.
[4] M.J. Rak, T. Friščića, A. Moores, Mechanochemical synthesis of Au, Pd, Ru and Re nanoparticles with lignin as a bio-based reducing agent and stabilizing matrix, Faraday Discuss. 170 (2014) 155–167.
[5] M. Maija-Liisa, J.J.V. Delgadoa, T. Leskinen, T. Anttila, G. Riviere, M. Sipponen, A. Paananen, K. Lintinen, M. Kostiainen, M. Österberg, Enzymatically and chemically oxidized lignin nanoparticles for biomaterial applications, Enzym. Microb. Technol. 111 (2018) 48–56.
[6] K.R. Aadil, A. Barapatre, S. Sahu, H. Jha, B.N. Tiwary, Free radical scavenging activity and reducing power of *Acacia nilotica* wood lignin, Int. J. Biol. Macromol. 67 (2014) 220–227.
[7] P. Figueiredo, K. Lintinen, A. Kiriazis, V. Hynninen, Z. Liu, T.B. Ramos, A. Rahikkala, A. Correia, T. Kohout, B. Sarmento, J. Yli-Kauhaluoma, J. Hirvonen, O. Ikkala, M.A. Kostiainen, H.A. Santos, In vitro evaluation of biodegradable lignin-based nanoparticles for drug delivery and enhanced antiproliferation effect in cancer cells, Biomaterials 121 (2017) 97–108.
[8] D. Kai, M.J. Tan, P.L. Chee, Y.K. Chua, Y.L. Yap, X.J. Loh, Towards lignin-based functional materials in a sustainable world, Green Chem. 18 (2016) 1175–1200.
[9] R.G. Saratale, H.-S. Shin, G. Kumar, G. Benelli, G.S. Ghodake, Y.Y. Jiang, D.S. Kim, G.D. Saratale, Exploiting fruit byproducts for eco-friendly nanosynthesis: *Citrus* × *clementina* peel extract mediated fabrication of silver nanoparticles with high efficacy against microbial pathogens and rat glial tumor C6 cells, Environ. Sci. Pollut. Res. 25 (2018) 10250–10263.
[10] R.G. Saratale, I. Karuppusamy, G.D. Saratale, A. Pugazhendhi, G. Kumar, Y. Park, G.S. Ghodake, R.N. Bharagava, J.R. Banu, H.S. Shin, A comprehensive review on green nanomaterials using biological systems: recent perception and their future applications, Colloids Surf. B: Biointerfaces 170 (2018) 20–35.
[11] R.G. Saratale, H.S. Shin, G. Kumar, G. Benelli, D.S. Kim, G.D. Saratale, Exploiting antidiabetic activity of silver nanoparticles synthesized using *Punica granatum* leaves and anticancer potential against human liver cancer cells (HepG2), Artif. Cells Nanomed. Biotechnol. 46 (2018) 211–222.
[12] G.D. Saratale, R.G. Saratale, G. Benelli, G. Kumar, A. Pugazhendhi, D.S. Kim, H.S. Shin, Anti-diabetic potential of silver nanoparticles synthesized with *Argyreia nervosa* leaf extract high synergistic antibacterial activity with standard antibiotics against foodborne bacteria, J. Clust. Sci. 28 (2017) 1709–1727.
[13] S. Hu, Y.L. Hsieh, Synthesis of surface bound silver nanoparticles on cellulose fibers using lignin as multi-functional agent, Carbohydr. Polym. 131 (2015) 134–141.
[14] M. Zimniewska, R. Kozłowski, J. Batog, Nanolignin modified linen fabric as a multifunctional product, Mol. Cryst. Liq. Cryst. 484 (2008) 409–416.
[15] T.T. Hanh, N.T. Thu, N.Q. Hien, P.N. An, T.T.K. Loan, P.T. Hoa, Preparation of silver nanoparticles fabrics against multidrug-resistant bacteria, Radiat. Phys. Chem. 121 (2016) 87–92.
[16] J. Shi, P.W. Kantoff, R. Wooster, O.C. Farokhzad, Cancer nanomedicine: progress, challenges and opportunities, Nat. Rev. Cancer 17 (2017) 20–37.
[17] S. Tran, P.J. DeGiovanni, B. Piel, P. Rai, Cancer nanomedicine: a review of recent success in drug delivery, Clin. Transl. Med. 6 (2017) 44.
[18] F. Meng, X. Yan, J. Liu, J. Gu, Z. Zou, Nanoporous gold as non-enzymatic sensor for hydrogen peroxide, Electrochim. Acta 56 (2011) 4657–4662.
[19] C.-Y. Lin, Y.-H. Lai, A. Balamurugan, R. Vittal, C.-W. Lin, K.-C. Ho, Electrode modified with a composite film of ZnO nanorods and Ag nanoparticles as a sensor for hydrogen peroxide, Talanta 82 (2010) 340–347.
[20] G.D. Saratale, M.Y. Jung, M.K. Oh, Reutilization of green liquor chemicals for pretreatment of whole rice waste biomass and its application to 2,3-butanediol production, Bioresour. Technol. 205 (2016) 90–96.
[21] G.D. Saratale, M.K. Oh, Characterization of poly-3-hydroxybutyrate (PHB) produced from *Ralstonia eutropha* using an alkali-pretreated biomass feedstock, Int. J. Biol. Macromol. 80 (2015) 627–635.
[22] J.E. Hedge, B.T. Hofreiter, R.L. Whistler, J.N. Miller (Eds.), Carbohydrates Chemistry, Academic Press, New York, NY 1962, p. 17.
[23] V.L. Singleton, R. Orthofer, Analysis of total phenols and other oxidation substrates and antioxidants by means of folin-ciocalteu reagent, Methods Enzymol. 299 (1999) 152–178.
[24] O. Goldschmidt, Determination of the phenolic hydroxyl content of lignin preparations by ultraviolet spectrometry, Anal. Chem. 26 (1954) 1421–1423.
[25] R.J.A. Gosselink, A. Abacherli, H. Semke, R. Malherbe, P. Kauper, A. Nadif, J.E.G. Van Dam, Analytical protocols for characterization of sulphur-free lignin, Ind. Crop. Prod. 19 (2004) 271–281.
[26] R.G. Saratale, G. Benelli, G. Kumar, D.S. Kim, G.D. Saratale, Bio-fabrication of silver nanoparticles using the leaf extract of an ancient herbal medicine, dandelion (*Taraxacum officinale*), evaluation of their antioxidant, anticancer potential, and antimicrobial activity against phytopathogens, Environ. Sci. Pollut. Res. 25 (2018) 10392–10406.
[27] K.R. Aadil, A. Barapatre, M. Avtar Singh, H. Jha, Hydrogen peroxide sensing and cytotoxicity activity of Acacia lignin stabilized silver nanoparticles, Int. J. Biol. Macromol. 82 (2016) 39–47.
[28] A.W. Bauer, W.M.M. Kirby, J.C. Sherris, M. Turck, Antibiotic susceptibility testing by a standardized single disk method, Am. J. Clin. Pathol. 45 (1966) 493–496.
[29] E. Filippo, A. Serra, D. Manno, Poly (vinyl alocohol) capped silver nanoparticles as localized surface plasmon resonance-based hydrogen peroxide sensor, Sensors Actuators B Chem. 138 (2009) 625–630.
[30] A. Garcia, A. Toledano, M.A. Andres, J. Labidi, Study of the antioxidant capacity of *Miscanthus sinensis* lignins, Process Biochem. 45 (2010) 935–940.
[31] N. Yang, W.H. Li, Mango peel extract mediated novel route for synthesis of silver nanoparticles and antibacterial application of silver nanoparticles loaded onto non-woven fabrics, Ind. Crop. Prod. 48 (2013) 81–88.
[32] S. Kanchi, G. Kumar, A.Y. Lo, C.M. Tseng, S.K. Chen, C.Y. Lin, T.S. Chin, Exploitation of de-oiled jatrophawaste for gold nanoparticles synthesis: a green approach, Arab. J. Chem. 11 (2018) 247–255.
[33] R.G. Saratale, G.D. Saratale, H.S. Shin, J.M. Jacob, A. Pugazhendhi, M. Bhaisare, G. Kumar, New insights on the green synthesis of metallic nanoparticles using plant and waste biomaterials: current knowledge, their agricultural and environmental applications, Environ. Sci. Pollut. Res. 25 (2018) 10164–10183.
[34] P. Kanmani, S.T. Lim, Synthesis and characterization of pullulan-mediated silver nanoparticles and its antimicrobial activities, Carbohydr. Polym. 97 (2013) 421–428.
[35] K.P. Bankura, D. Maity, M.M.R. Mollick, D. Mondal, B. Bhowmick, M.K. Bain, A. Chakraborty, J. Sarkar, K. Acharya, D. Chattopadhyay, Synthesis, characterization and antimicrobial activity of dextran stabilized silver nanoparticles in aqueous medium, Carbohydr. Polym. 89 (2012) 1159–1165.
[36] S. Mohan, O.S. Oluwafemi, S.C. George, V.P. Jayachandran, F.B. Lewu, S.P. Songca, N. Kalarikkal, S. Thomas, Completely green synthesis of dextrose reduced silver nanoparticles, its antimicrobial and sensing properties, Carbohydr. Polym. 106 (2014) 469–474.
[37] T.C. Prarthna, N. Chandrasekaran, M. Raichur, A. Mukherjee, Biomimetic synthesis of silver nanoparticles by *Citrus limon* (lemon) aqueous extract and theoretical prediction of particle, Colloids Surf. B: Biointerfaces 82 (2011) 152–159.
[38] Z.U.H. Khan, A. Khan, Y.C.N.S. Shah, N. Muhammad, A.U. Khan, K.T.F.U. Khan, B. Murtaza, S.U.H.S.A. Qaisrani, P. Wan, Biomedical applications of green synthesized Nobel metal nanoparticles, J. Photochem. Photobiol. B 173 (2017) 150–164.
[39] R. Sathiya Priya, D. Geetha, P.S. Ramesh, Antioxidant activity of chemically synthesized AgNPs and biosynthesized *Pongamia pinnata* leaf extract mediated AgNPs – a comparative study, Ecotoxicol. Environ. Saf. 134 (2016) 308–318.
[40] G.S. Ghodake, S.K. Shinde, R.G. Saratale, A.A. Kadam, G.D. Saratale, A. Syed, F. Ameen, D.Y. Kim, Colorimetric detection of Cu2+ based on the formation of peptide–copper complexes on silver nanoparticle surfaces, Beilstein J. Nanotechnol. 9 (2018) 1414–1422.
[41] J. Cai, W. Xu, Y. Liu, Z. Zhu, G. Liu, W. Ding, G. Wang, H. Wang, Y. Luo, Robust construction of flexible bacterial cellulose@Ni$(OH)_2$ paper: toward high capacitance and sensitive H_2O_2 detection, Eng. Sci. (2018)https://doi.org/10.30919/es8d669.
[42] S. Raja, R. Vinayagam, T. Varadavenkatesan, Green biosynthesis of silver nanoparticles using *Calliandra haematocephala* leaf extract, their antibacterial activity and hydrogen peroxide sensing capability, Arab. J. Chem. 10 (2017) 253–261.